Transient Photoresponse of the Tris(2,2′-bipyridine)ruthenium(II)-Catalyzed Minimal Bromate Oscillator

Akiko Kaminaga

Institute for Molecular Science, Myodaiji, Okazaki 444, Japan

Ichiro Hanazaki*

Department of Chemistry, Faculty of Science, Hiroshima University, 1-3-1 Kagamiyama, Higashi-Hiroshima 739, Japan

Received: January 5, 1998

The tris(2,2′-bipyridine)ruthenium(II)-catalyzed minimal bromate oscillator under flow conditions was found to exhibit various dynamical responses to the pulsed-light perturbation in the visible region. The system in its reduced steady state exhibits excitability with a threshold in the applied light-pulse energy, while the oxidized steady state does not respond to the light pulse. The latter exhibits, however, a slow response without a threshold to the negative light pulse. The system in its oscillatory state exhibits a phase shift of oscillations upon application of a pulsed-light perturbation. The oscillation phase is mostly advanced or unaffected, depending on the phase of application of the light pulse, although a narrow region of phase delay has also been found in between. A phase portrait spanned by the redox potential and the bromide ion-selective electrode potential has been determined experimentally on the basis of which the system dynamics is discussed in detail. All these results suggest the importance of the photoproduction of extra $HBrO_2$ upon pulsed-light illumination to induce the autocatalytic process that forces the system to experience a single turn along the limit cycle. A numerical calculation based on the Noyes−Field−Thompson model has supported the proposed features, demonstrating that the pulsed addition of $HBrO_2$ reduces the concentration of Br^- quickly. When it is reduced below a certain threshold value, the autocatalytic growth of $HBrO_2$, as well as of the catalyst in its oxidized form, is initiated to exhibit the response corresponding to the observation.

Introduction

Among several chemical oscillators, the Belousov−Zhabotinsky (BZ) reaction is known to exhibit a variety of nonlinear phenomena such as spatial pattern formation and chaotic oscillations in addition to normal sustained oscillations. By use of a photosensitive catalyst such as the tris(2,2′-bipyridine)-ruthenium(II) ion (hereafter abbreviated $Ru(bpy)_3^{2+}$), it exhibits some interesting responses to light, such as the photoinduction and -inhibition of oscillations in the homogeneous system and the photoassisted spatial pattern formation in the inhomogeneous system. Its photoresponse has attracted considerable attention, since light is an excellent external control parameter for its facility in controlling intensity as well as wavelength.[1] However, the mechanistic aspects of the photoresponse are fairly complicated and are still in controversy.

In the case of steady illumination of the $Ru(bpy)_3^{2+}$-catalyzed BZ system, which exhibits photoinduction and -inhibition of oscillations, the primary light absorber has been confirmed to be $Ru(bpy)_3^{2+}$.[2,3] For photoinduction of oscillations, we have proposed the photoproduction of $HBrO_2$ as a key step:[4,5]

$$*Ru(bpy)_3^{2+} + Ru(bpy)_3^{2+} + BrO_3^- + 3H^+ \rightarrow 2Ru(bpy)_3^{3+} + HBrO_2 + H_2O \quad (1)$$

where $*Ru(bpy)_3^{2+}$ is the photoexcited catalyst.

In the dark reactions 2−4 are known to be important in determining the nonlinear behavior of the system:[6]

$$BrO_3^- + HBrO_2 + H^+ \rightarrow 2BrO_2^\bullet + H_2O \quad (2)$$

$$Ru(bpy)_3^{2+} + BrO_2^\bullet + H^+ \rightarrow Ru(bpy)_3^{3+} + HBrO_2 \quad (3)$$

$$HBrO_2 + Br^- + H^+ \leftrightarrow 2HOBr \quad (4)$$

If $[Br^-]$ is large, rapid reaction 4 keeps $[HBrO_2] \approx 0$, where reaction 2 never proceeds and the system stays in the reduced steady state (SSI). If $[Br^-]$ decreases below a certain threshold $[Br^-]_{th}$, reaction 2 starts to give the autocatalytic process 5 ≡ reaction 2 + 2(reaction 3):

$$2Ru(bpy)_3^{2+} + BrO_3^- + HBrO_2 + 3H^+ \rightarrow 2Ru(bpy)_3^{3+} + 2HBrO_2 + H_2O \quad (5)$$

where reaction 2 is rate-determining. This brings the system into the oscillatory state (OSC). The photoinduction of oscillations should occur if excess $HBrO_2$ produced by reaction 1 reduces $[Br^-]$ below $[Br^-]_{th}$ through reaction 4. The photoproduction of $HBrO_2$ in reaction 1 may also be written as

$$*Ru(bpy)_3^{2+} + BrO_3^- + 2H^+ \rightarrow Ru(bpy)_3^{3+} + BrO_2^\bullet + H_2O \quad (6)$$

* To whom correspondence should be addressed. E-mail: hanazaki@sci.hiroshima-u.ac.jp.

S1089-5639(98)00618-5 CCC: $15.00
Published on Web 04/18/1998

which forms reaction 1 if it is combined with reaction 3: reaction 1 ≡ reaction 6 + reaction 3.

On the other hand, for the photoinhibition of oscillations in the full BZ system with malonic acid as a substrate, the photoproduction of Br^- has been believed to be effective by bringing the system into SSI. However, it is not quite clear how excess Br^- is photoproduced. Kuhnert has proposed the following scheme in relation to the photocontrolled spatial pattern formation:[7]

$$6^*Ru(bpy)_3^{2+} + BrO_3^- + 6H^+ \rightarrow 6Ru(bpy)_3^{3+} + 3H_2O + Br^- \quad (7)$$

It is, however, quite unrealistic, since it requires six photoexcited catalysts to react. We have proposed a more plausible scheme[4]

$$^*Ru(bpy)_3^{2+} + 3Ru(bpy)_3^{2+} + HBrO_2 + 3H^+ \rightarrow 4Ru(bpy)_3^{3+} + 2H_2O + Br^- \quad (8)$$

which is thermochemically feasible and effective in inhibiting oscillations, since it produces Br^- and consumes $HBrO_2$ simultaneously. Yamaguchi and co-workers[8] have recently suggested that the decomposition of bromomalonic acid in the reaction with $Ru(bpy)_3^{3+}$ or $Ru(bpy)_3^{+}$ produced from $^*Ru(bpy)_3^{2+}$ could be a source of Br^-.

The reaction mechanisms of nonlinear processes are very complicated in general, and it is sometimes difficult to obtain sufficient experimental information to establish the mechanism. Study of the response of the system to a pulsed perturbation gives us an opportunity to obtain additional experimental information. Marek and co-workers have reported such an experiment by adding a drop of solution containing Br^- or Ag^+ to the dark BZ system.[9] The response of the system to a light pulse should be more interesting to study in view of the feasibility in controlling its energy, pulse duration, and also wavelength. A few such examples have been reported, including studies of the photoinduced phase delay of oscillations,[4,10] quenching near a bifurcation point,[11] and the periodic stimulation of spiral waves.[12] We have recently reported preliminary results of the response of some chemical oscillator systems to a light pulse, including the $Ru(bpy)_3^{2+}$-catalyzed BZ system,[13] the $Ru(bpy)_3^{2+}$-catalyzed minimal bromate oscillator (MBO),[14] and the ferrocyanide−hydrogen peroxide−sulfite system.[15] It has been found that the study of the response of these systems to the pulse light is useful in understanding the photoassisted nonlinear phenomena in more detail.

In this paper, we present a full account of our recent study of the response of the MBO system to the pulsed-light perturbation. The MBO system contains no organic substrate such as malonic acid, giving us the advantage of avoiding complicated organic reactions involved in the full BZ system. With this choice, we expect to obtain much deeper insight of the phenomena than those obtained previously. We have also performed numerical calculations to confirm the proposed mechanism for the photoresponse of this system.

Experimental Section

Reagent grade $NaBrO_3$ and NaBr (Wako Pure Chemical) and H_2SO_4 (Katayama Chemical) were used without further purification. $Ru(bpy)_3SO_4$ was prepared from $Ru(bpy)_3Cl_2 \cdot 6H_2O$ (Aldrich) by reprecipitation in 3 M sulfuric acid in order to make it free from chloride ions.[16] Freshly prepared solutions in distilled water were pumped into a cell separately through inlet tubes by a peristaltic pump (Eyela, MP-3) and stirred rigorously with a Teflon coated magnetic stirrer bar. Initial concentrations (the concentration that would be realized in the cell if no reaction took place) were fixed at $[Ru(bpy)_3^{2+}]_0 = 0.1$ mM, $[BrO_3^-]_0 = 25$ mM, and $[H_2SO_4]_0 = 0.80$ M. A double-jacketed acryl resin cell was thermostated at 25 °C. The cell was equipped with a combined platinum electrode (Metrohm, No. 916-0408-100), a bromide ion selective electrode (Toa, BR-125), and quartz windows for illumination (optical path length = 2 cm). A 500 W Hg lamp (Ushio, USH-500D) with an L39 filter and a set of neutral density filters (Hoya) was used as a light source, providing major lines at $\lambda = 395$, 405, 436, 545, and 577 nm in the visible region. The light power was monitored by a photodiode (Hamamatsu, S1723-05). The maximum light power (P_{max}) at the incident cell window was typically 1.30 W.

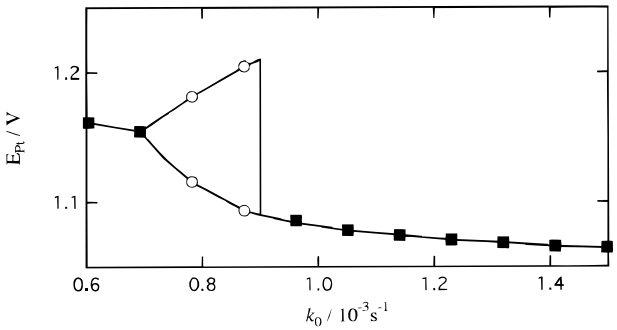

Figure 1. Bifurcation diagram for MBO under the dark condition. A pair of open circles for a single k_0 indicate the maximum and minimum values of the redox potential in oscillations, and the squares indicate the values for the steady states. Initial concentrations are $[Ru(bpy)_3^{2+}]_0 = 0.10$ mM, $[BrO_3^-]_0 = 25$ mM, $[Br^-]_0 = 0.25$ mM, and $[H_2SO_4]_0 = 0.80$ M.

Results and Discussion

The MBO system is known as one of the flow-controlled oscillators, which requires external supply of Br^- to exhibit oscillations, since it has no effective internal source of Br^-. Figure 1 shows a bifurcation diagram for the $Ru(bpy)_3^{2+}$-catalyzed MBO in the dark, taking the flow rate as an external control parameter. The flow rate is expressed in the normalized form defined by $k_0 \equiv v/V$, where v is the total flow rate (mL s^{-1}) and V is the cell volume (12 mL). Figure 1 shows that the system bifurcates from SSI to OSC when k_0 is decreased. A further decrease of k_0 induces another bifurcation from OSC to the oxidized steady state (SSII). A decrease of k_0 should cause a reduced external supply of Br^- and an extended residence time of the materials in the cell, which causes the autocatalytic process to occur more easily.

The photoresponse of MBO with $Ru(bpy)_3^{2+}$ as a catalyst has been examined under the steady illumination and found to show photoinduction and -inhibition of oscillations.[17] A bifurcation diagram of this system, taking the incident light power (P) as an external control parameter, is given in Figure 2. The steady illumination of the system in SSI with visible light causes a bifurcation into OSC for P beyond a critical value. This behavior for the steady illumination can be understood as follows. For illumination in SSI, extra $HBrO_2$ photoproduced through reaction 1 reduces $[Br^-]$ through reaction 4. If $[Br^-]$ decreases below $[Br^-]_{th}$, autocatalytic reaction 5 starts to cause a bifurcation into OSC. A further increase of P causes another bifurcation from OSC to SSII. Roughly speaking, this is

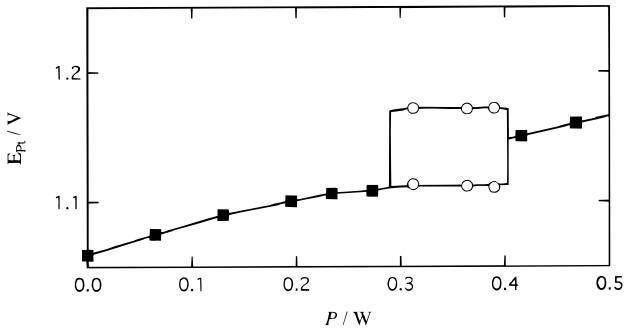

Figure 2. Bifurcation diagram for MBO under the steady light irradiation. A pair of open circles for a single P indicate the maximum and minimum value of the redox potential in oscillations, and the squares indicate the values for the steady state. Initial concentrations are the same as those in Figure 1. $k_0 = 1.05 \times 10^{-3}$ s^{-1}.

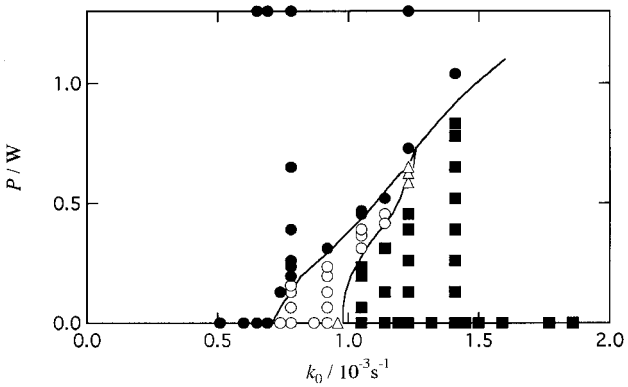

Figure 3. State diagram in the k_0-P plane for the MBO system under steady illumination: (○) OSC; (△) irregular oscillatory; (■) SSI; (●) SSII. Initial concentrations are the same as those in Figure 1.

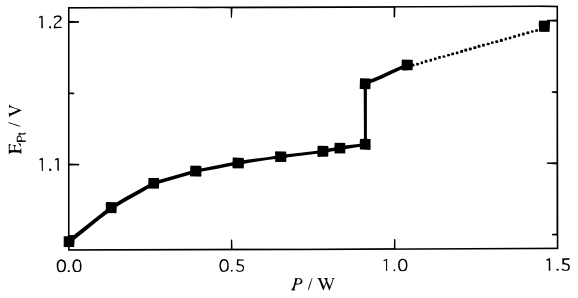

Figure 4. Variation of E_{Pt} with P. Initial concentrations are the same as those in Figure 1. $k_0 = 1.46 \times 10^{-3}$ s^{-1}. The point for $P = 1.30$ W has been estimated by an extrapolation of the results for $P = 1.30$ W in Figure 3 with respect to k_0.

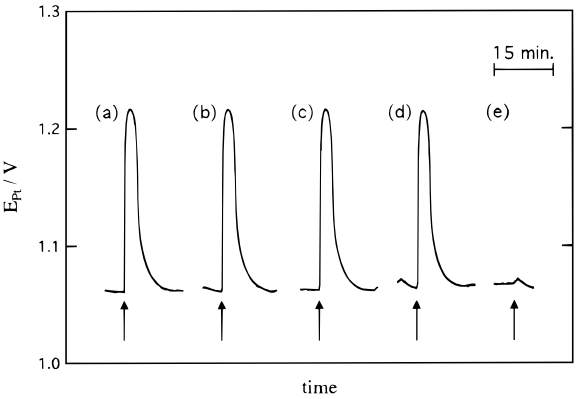

Figure 5. Time profile of the redox potential for the MBO system in SSI after a single pulsed-light irradiation. The arrows indicate the time of pulse illumination. $P\tau = 1.30$ W × 1 s (a), 1.30 W × 0.5 s (b), 0.65 W × 1 s (c), 0.325 W × 2 s (d), and 0.325 W × 1 s (e). Initial concentrations are the same as those in Figure 1. $k_0 = 1.05 \times 10^{-3}$ s^{-1}.

because the increased rate of photoproduction of $HBrO_2$ makes $[Br^-]$ always lower than $[Br^-]_{th}$. It is also noted that, at the extreme of $P \rightarrow \infty$, the increased rate of photoproduction of $HBrO_2$ and decreased $[Ru(bpy)_3^{2+}]$ cause a shift of the rate-determining step from reaction 2 to reaction 3, where $BrO_2^\bullet$ photoproduced by reaction 6 is piled up and a preequilibrium holds for reaction 2. No "threshold" behavior is expected in this situation. Most of the $Ru(bpy)_3^{2+}$ is converted to $Ru(bpy)_3^{3+}$, and a small amount of $Ru(bpy)_3^{2+}$ and a relatively large amount of $BrO_2^\bullet$ keep the rate of formation of $Ru(bpy)_3^{3+}$ by reaction 3 to be balanced with the rate of flow-out of $Ru(bpy)_3^{3+}$ from the cell.

Figure 3 is a state diagram spanned by P and k_0 in which a narrow region of OSC is sandwiched in SSI and SSII. At higher k_0, the OSC region disappears. In a typical state diagram of cross-shaped type, a bistable region is expected to exist above the crossing point of the two bifurcation curves.[18] In the present case, however, no indication of bistability has been detected experimentally, while a stepwise variation of the redox potential (E_{Pt}) has been observed between SSI and SSII upon an increase of P as illustrated in Figure 4. This "jump" of E_{Pt} should be a border between SSI and SSII as indicated in Figure 3, corresponding to the change of the rate-determining step discussed above.

Figure 5 illustrates some typical responses of MBO in SSI in the dark to a single light-pulse perturbation. The system gives a pulse response only for $P > P_c$, where P_c is a certain critical value of P. P_c has been determined for various pulse duration times τ and found to be inversely proportional to τ, as $P_c\tau = 0.65$ J.[14] This means that the threshold is determined by the total pulse energy, not by the peak power. The amplitude of the response is independent of P above P_c. These observations suggest that the system is excitable in SSI.

The excitable behavior is reasonably understood on the basis of reactions 4 and 5 combined with reaction 1. Namely, a threshold exists in the light pulse energy because it is required for the firing of autocatalysis 5 to produce a sufficient amount of $HBrO_2$ by reaction 1 to make $[Br^-] < [Br^-]_{th}$ through reaction 4. The independence of the peak height of the response to the light energy is due to the fact that once the autocatalysis is fired, the system experiences a single complete turn along the limit cycle for the dark oscillations.

In contrast to SSI, no response has been observed in the present experiment to a pulsed illumination of the system in SSII up to the maximum available pulse energy.[14] This should partly be due to the lower concentration of $Ru(bpy)_3^{2+}$ in SSII, which is the primary light absorber. However, we should also consider the changeover of the rate-determining step from reaction 2 in SSI to reaction 3 in SSII, for which no "threshold" nature is expected any more. Although an increase of the intensity of steady illumination in SSII results in an increase of the steady concentration of $Ru(bpy)_3^{3+}$, the system is insensitive to the pulsed perturbation.

We have also examined the effect of a "negative pulse", which is created by cutting the steady illumination off for a short period τ, when the system stays in SSII. Figure 6 shows a few examples for the system initially in SSII, where a sudden decrease of P down to 0 for $\tau = 1.0$ s gives no response, while the 10 s pulse gives a negative pulse response in the redox

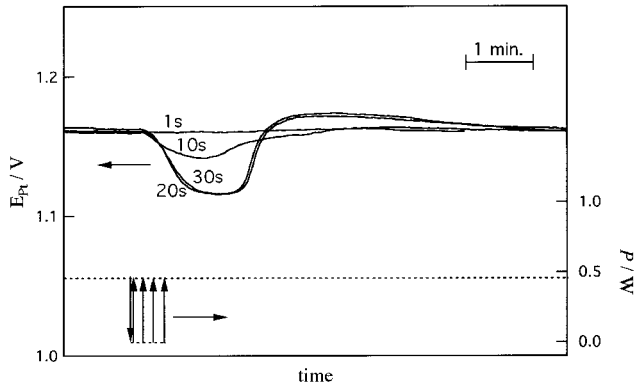

Figure 6. Response of MBO to a pulsed cutoff of the steady illumination in SSII. The lower part shows the temporal change of light power P, which is instantaneously decreased to 0 from its steady value of $P = 0.47$ W for an interval of $\tau = 1.0$, 10, 20, or 30 s. Initial concentrations are the same as those in Figure 1. $k_0 = 1.05 \times 10^{-3}$ s^{-1}.

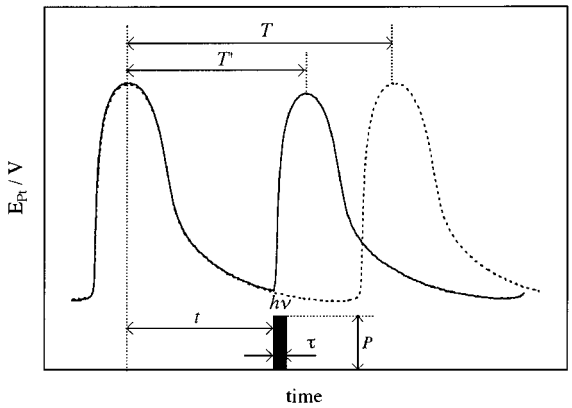

Figure 7. Single light-pulse perturbation on the oscillatory MBO system. The broken curve shows the oscillations with the period T in the dark. The light pulse of duration τ and intensity P is applied at time t to cause a phase shift.

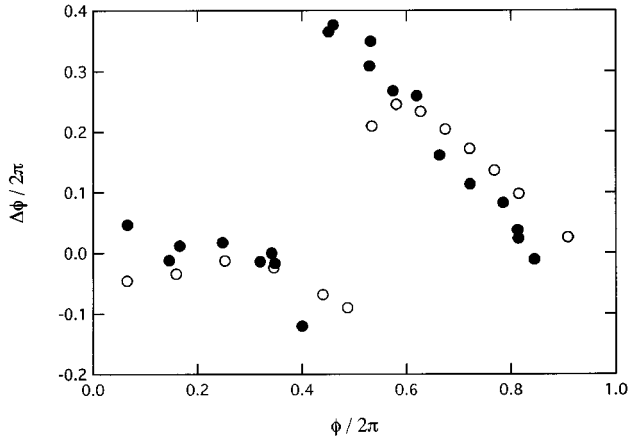

Figure 8. Experimental (●) and calculated (○) phase shifts $\Delta\phi$ vs the phase ϕ of application of a pulse light. In the experiment, the light pulse of $P = 1.30$ W and $\tau = 1.0$ s has been applied. Initial concentrations are the same as those in Figure 1. $k_0 = 0.78 \times 10^{-3}$ s^{-1}. Calculated results are for $\Delta[HBrO_2] = 1.5 \times 10^{-7}$ M and $k_0 = 1.63 \times 10^{-3}$ s^{-1}.

potential. In this case, E_{Pt} comes down but does not reach the value corresponding to the OSC region (Figure 2), giving a smooth return to the initial value. The response increases with increasing τ and seems to saturate at $\tau \geq 20$ s. For $\tau \geq 20$ s, the negative pulse response is followed by an overshoot. The maximum and minimum of the amplitude correspond to the amplitude of oscillations in the OSC region (Figure 2), suggesting that the system undergoes a single turn along the limit cycle. The minimum value of E_{Pt} in the negative response in the case of $\tau \geq 20$ s corresponds to the lowest E_{Pt} value in the OSC region, where an oscillatory recovery of E_{Pt} occurs to give the overshoot (or the relaxation oscillations).

The appearance of the overshoot may be understood as follows. If we pay attention to the overshoot alone, it appears with a threshold with respect to τ above which the amplitude of overshoot is constant; namely, it looks like an excitable response. This is because E_{Pt} does not come down sufficiently for a smaller τ so that the system retains the SSII character, while for a larger τ, it comes down to the value corresponding to SSI, where the recovery of the light intensity at the end of the negative pulse triggers autocatalysis 5 with a threshold to force the system to experience a single turn along the limit cycle. Therefore, the overshoot is the same response as that for the system in SSI; a prolonged negative pulse brings the system to SSI, which exhibits the normal excitable response at the end of the light pulse.

Besides the overshoot, the essential response to a negative pulse shows no excitable behavior, since the reaction scheme taking place in SSII has no threshold as mentioned above. In addition, the response to the negative pulse starts to appear with a delay of ca. 10 s and the rise time of the negative signal is ca. 50−70 s/0.1 V, compared with ca. 10 s/0.1 V for the positive response in SSI. The slower response is due to the absence of autocatalysis in the negative response. In addition, we are observing the redox potential that is determined by $[Ru(bpy)_3^{3+}]/[Ru(bpy)_3^{2+}] = \rho/(1 - \rho)$, where $\rho \equiv [Ru(bpy)_3^{3+}]/[Ru(bpy)_3^{2+}]_0$. Although the cutoff of the illumination reduces the rate of formation of $Ru(bpy)_3^{3+}$, there is no effective reaction to reduce $[Ru(bpy)_3^{3+}]$ internally so that it decreases rather slowly according to the rate of flow out of the solution from the reaction cell.

We have also examined the effect of a single pulse light on MBO in OSC. The shift of the oscillation phase is observed depending on the phase of the pulse light application as shown in Figure 7, which illustrates a typical phase advance of oscillations. The phase of the pulsed-light application ϕ and the phase shift of oscillations $\Delta\phi$ are defined as

$$\phi = 2\pi t/T \tag{9}$$

$$\Delta\phi = 2\pi(T - T')/T \tag{10}$$

where T is the period of the dark oscillations, T' is the period right after the pulsed-light application, and t is the time of application of the pulse light.

The observed results are summarized in a phase-response diagram as shown in Figure 8, where $\Delta\phi$ is given as a function of ϕ (●). The figure shows clearly that the "excitable" phase ($\Delta\phi > 0$; phase-advanced) exists for the region $0.45 \leq \phi/(2\pi) < 1.0$, in which the system responds immediately after the light pulse. There is also the "refractory" phase for $0 < \phi/(2\pi) < 0.4$, in which no response is observed in the pulsed-light perturbation ($\Delta\phi \approx 0$). The two phases are separated by a narrow region of $\Delta\phi < 0$ (phase-delayed) at $f/(2\pi) \approx 0.4$.

To see the dynamics involved in the photoresponse in more detail, we have constructed a two-dimensional phase portrait spanned by the redox potential (E_{Pt}) and the bromide ion selective electrode potential (E_{Br^-}) as shown in Figure 9. Note

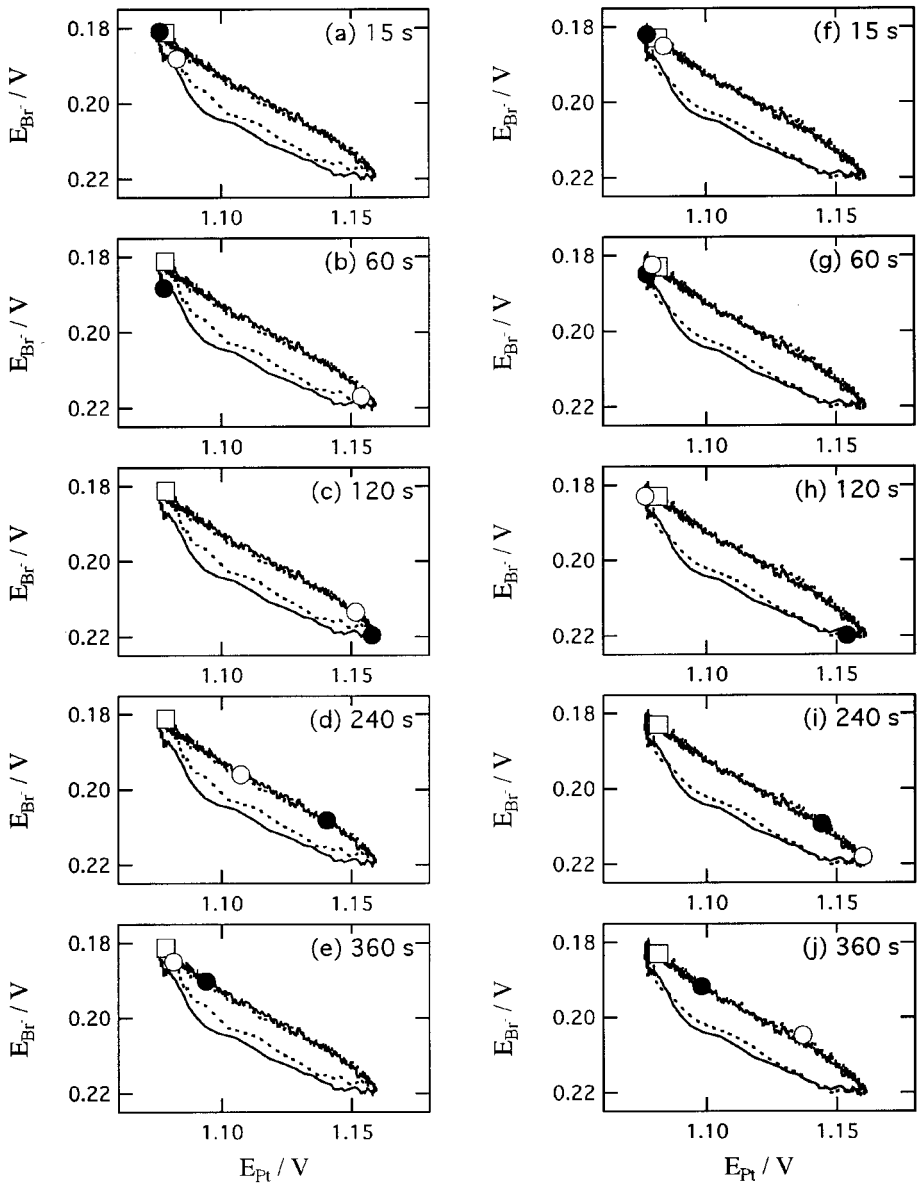

Figure 9. Phase portraits for MBO experimentally determined in the dark oscillations (● and solid curve) and in the phase-shifted oscillations (○ and broken curve). The time of application of the light pulse ($P = 1.30$ W and $\tau = 1.0$ s) is indicated by an open square. Panels a−e are for the phase-advanced case, and panels f−j are for the phase-delayed case. The time after the pulse application is indicated in each panel. Initial concentrations are the same as those in Figure 1 except for $[Br^-]_0 = 0.30$ mM. $k_0 = 0.78 \times 10^{-3}$ s^{-1}.

that E_{Br^-} is plotted in decreasing order so that an increase in the ordinate corresponds to an increase in $[Br^-]$. In constructing the phase portrait, we have encountered a difficulty due to the slow response of the bromide ion selective electrode, which would affect the measured time evolution considerably. To eliminate it, we have corrected the observed time response for the response time of the electrode ($\tau_e = 0.74$ min) assuming an exponential-type time delay (see Appendix). In Figure 9, the representative point for the dark oscillations is shown by a filled circle, which moves along the limit cycle (solid curve) counterclockwise. The upper half of the limit cycle corresponds to a slow decrease of E_{Pt} down from the peak (see Figure 7), while the lower half corresponds to a rapid rise due to the autocatalytic oxidation of the system.

A pulsed-light is applied at the point indicated by an open square. The open circle represents the system after the pulse illumination. In the refractory phase, the system continues to travel along the limit cycle corresponding to the dark oscillations without being affected by the pulse irradiation. On the other hand, in the phase-advanced case (parts a−e of Figure 9), the pulsed perturbation initiates autocatalysis immediately to create a shortcut in the limit cycle (broken curve), resulting in a shorter period of the first single cycle after the pulse illumination. After a single turn along the shortcut, the system returns to the dark limit cycle (solid curve). Parts f−j of Figure 9 show the phase-delayed case, where the system right after the light pulse moves slightly backward along the limit cycle (clockwise) as seen in Figure 9f. It then comes back to the starting point (Figure 9g) and continues the normal movement in the dark without creating a new locus (parts h−j of Figure 9). This "hesitation" takes extra time, resulting in the observed phase delay.

For the purpose of confirming the mechanism of photoresponse of MBO proposed here, we have performed some numerical calculations based on the Noyes−Field−Thompson (NFT) model,[19,20] which is known to reproduce the experimental results for the cerium ion-catalyzed MBO very well. The reaction scheme is

$$BrO_3^- + Br^- + 2H^+ \leftrightarrow HBrO_2 + HOBr \quad (N1)$$

$$HBrO_2 + Br^- + H^+ \leftrightarrow 2HOBr \quad (N2)$$

$$BrO_3^- + HBrO_2 + H^+ \leftrightarrow 2BrO_2^\bullet + H_2O \quad (N3)$$

$$Ru(bpy)_3^{2+} + BrO_2^\bullet + H^+ \rightarrow Ru(bpy)_3^{3+} + HBrO_2 \quad (N4)$$

$$HOBr + Br^- + H^+ \leftrightarrow Br_2 + H_2O \quad (N5)$$

$$2HBrO_2 \leftrightarrow BrO_3^- + HOBr + H^+ \quad (N6)$$

where reaction N2 ≡ reaction 4, reaction N3 ≡ reaction 2, and reaction N4 ≡ reaction 3. The rate constants for this model given by Field and Försterling[21] are summarized in Table 1 except for those for reactions N3 and N4. Their rate constant for the forward reaction of process N3, $k_{N3} = 42\ M^{-2}\ s^{-1}$ has been increased to $65\ M^{-2}\ s^{-1}$ to reproduce the present results. The rate constant for reaction N4, $k_{N4} = 4 \times 10^6\ M^{-2}\ s^{-1}$, determined for the $Ru(bpy)_3^{2+}$-catalyzed full BZ system by Gao et al.,[22] has been reduced to $1 \times 10^6\ M^{-2}\ s^{-1}$. According to Robertson et al.,[23] the actual $[H^+]$ in the 0.7754 M sulfuric acid aqueous solution is 0.992 M. We have therefore used $[H^+] = 1.0$ M in the present calculation, since $[H_2SO_4]_0 = 0.80$ M has been used in our experiments. Calculations have been carried out with a semiimplicit Runge−Kutta method.[24]

To simulate the pulse response of MBO, we have employed the method of "concentration pulse" in which the concentration of a key species (say, $HBrO_2$ or Br^-) is increased or decreased instantaneously for 1 s corresponding to the duration of pulsed-light perturbation. Figure 10 illustrates the calculated time evolutions of $[Ru(bpy)_3^{3+}]$ for the system in SSI. Figure 10A illustrates the effect of increasing $[HBrO_2]$. The system does not respond to the increase of $\Delta[HBrO_2] = 1 \times 10^{-7}$ M (curve a of Figure 10A), while almost the same response appears for $\Delta[HBrO_2] = 2 \times 10^{-7}$ M and 1×10^{-6} M (curves b and c, respectively), suggesting its excitable nature. An excitable response is seen also for $\Delta[Br^-] < 0$ (Figure 10D), as expected from the reaction scheme, in which a decrease of $[Br^-]$ below $[Br^-]_{th}$ initiates the autocatalytic oxidation of the system. No response is observed for $\Delta[HBrO_2] < 0$ (Figure 10B) or for $\Delta[Br^-] > 0$ (Figure 10C), which is again reasonable in view of the scheme.

The concentration pulse of $\Delta[HBrO_2] = 1.5 \times 10^{-7}$ M applied to MBO in OSC gives the oscillation phase shift as shown in Figure 8 by open circles, which are in reasonable agreement with the experiments given by filled circles. The calculated phase portraits are shown in Figure 11, which are spanned by $[Ru(bpy)_3^{3+}]$ and $[Br^-]$ instead of E_{Pt} and E_{Br^-} in Figure 9. The pulse perturbation is applied at the point indicated by an open square. In the phase-advanced case (Figure 11a), the pulsed perturbation initiates autocatalytic process immediately to create a shortcut. In the phase-delayed case (Figure 11b), the system right after the perturbation deviates from the limit cycle to the direction of reduced $[Br^-]$ but comes back soon to continue the normal movement. The calculation was made for an artificial increase of $[HBrO_2]$ not accompanied by the creation of $Ru(bpy)_3^{3+}$ as involved in the real reaction. However, as can be seen in Figure 8, the calculation reproduces the observed phase shift fairly well. This would suggest that the decrease of $[Br^-]$, not the increase of $[Ru(bpy)_3^{3+}]$, due to the extra $HBrO_2$ photoproduced by reaction 1 is important for determining the phase shift.

TABLE 1: Rate Constants Used in the Calculations[19]

	rate constants	
reaction	forward	reverse
N1	$2.0\ M^{-3}\ s^{-1}$	$3.2\ M^{-1}\ s^{-1}$
N2	$3 \times 10^6\ M^{-2}\ s^{-1}$	$2 \times 10^{-5}\ M^{-1}\ s^{-1}$
N3	$65\ M^{-2}\ s^{-1}$	$4.2 \times 10^7\ M^{-1}\ s^{-1}$
N4	$1 \times 10^6\ M^{-2}\ s^{-1}$	
N5	$8 \times 10^9\ M^{-2}\ s^{-1}$	$1.1 \times 10^2\ s^{-1}$
N6	$3 \times 10^3\ M^{-1}\ s^{-1}$	$1 \times 10^{-8}\ M^{-2}\ s^{-1}$

An analysis of the calculated results for the dark oscillations suggests that the external supply of Br^- with $[Br^-]_0 = 0.25$ mM and $k_0 = 1.63 \times 10^{-3}\ s^{-1}$ gives an increase of 0.41 mM s^{-1} of $[Br^-]$, corresponding to the external supply of ca. 260 mM of Br^- in a single period of oscillations. Most of the Br^- is, however, stored in the system in another form such as Br_2, while only less than 1% of them exist as Br^- ($[Br^-] \approx 0-1$ mM) during the oscillation. Br_2 could be a source of regeneration of Br^- through a relatively fast back-reaction of reaction N5. The calculated dark limit cycle in Figure 11 shows that $[Br^-]$ is recovered rather quickly to its maximum value after the oscillation peak is passed. Then, it decreases gradually to $[Br^-]_{th} \approx 0.8$ mM at the left end of the limit cycle where autocatalysis starts. The $\Delta[HBrO_2]$ pulse applied on the right half of the limit cycle, where $[Br^-]$ is rapidly increasing, gives no effect, since the autocatalytic reaction is still operating in this region. For the $[Br^-] > [Br^-]_{th}$ region, where $[Br^-]$ is gradually decreasing toward the bottom of the oscillation, the $\Delta[HBrO_2]$ pulse decreases $[Br^-]$ below $[Br^-]_{th}$ to initiate autocatalysis as shown in Figure 11a, creating a shortcut in the limit cycle. If the same $\Delta[HBrO_2]$ pulse is applied at an earlier stage, the increase in $[HBrO_2]$ is insufficient to decrease $[Br^-]$ below $[Br^-]_{th}$ and a slight decrease in $[Br^-]$ is instantaneously recovered by regeneration from Br_2, giving no appreciable effect in the oscillation phase. At an intermediate point (Figure 11b), $[Br^-]$ decreases appreciably but is still insufficient to start autocatalysis, taking an additional time before the system returns to the dark limit cycle. This would give a slight delay in the oscillation phase. A larger $\Delta[HBrO_2]$ pulse gives the initiation of autocatalysis at an earlier point on the limit cycle (namely, at smaller ϕ).

Conclusion

The response of the $Ru(bpy)_3^{2+}$-catalyzed minimal bromate oscillator in the flow system to the pulsed-light perturbation has been studied in this paper. The results, together with those in preliminary reports published earlier,[14,17] have established the mechanism of photoresponse of this system that could account for the steady as well as pulsed illumination consistently. The direct effect of illumination was confirmed to be the photoexcitation of $Ru(bpy)_3^{2+}$ followed by the production of extra $HBrO_2$ through reaction 1. The extra $HBrO_2$ reduces $[Br^-]$ below $[Br^-]_{th}$ through process 4 to induce autocatalytic reaction 5, resulting in a sharp excitable response when the light pulse is applied to the system in SSI. If the system in OSC is perturbed with a light pulse, the phase shift of oscillations is observed depending on the phase of the pulsed-light application. Although there is a narrow region of phase delay, the response is mostly phase-advanced. These photoinduced phase shifts can also be accounted for by the photoproduction of $HBrO_2$ mentioned above. The MBO system in the oxidized steady state (SSII) does not give any appreciable response to the (positive) light pulse up to the maximum pulse energy employed here. It exhibits, however, a delayed response without threshold to the

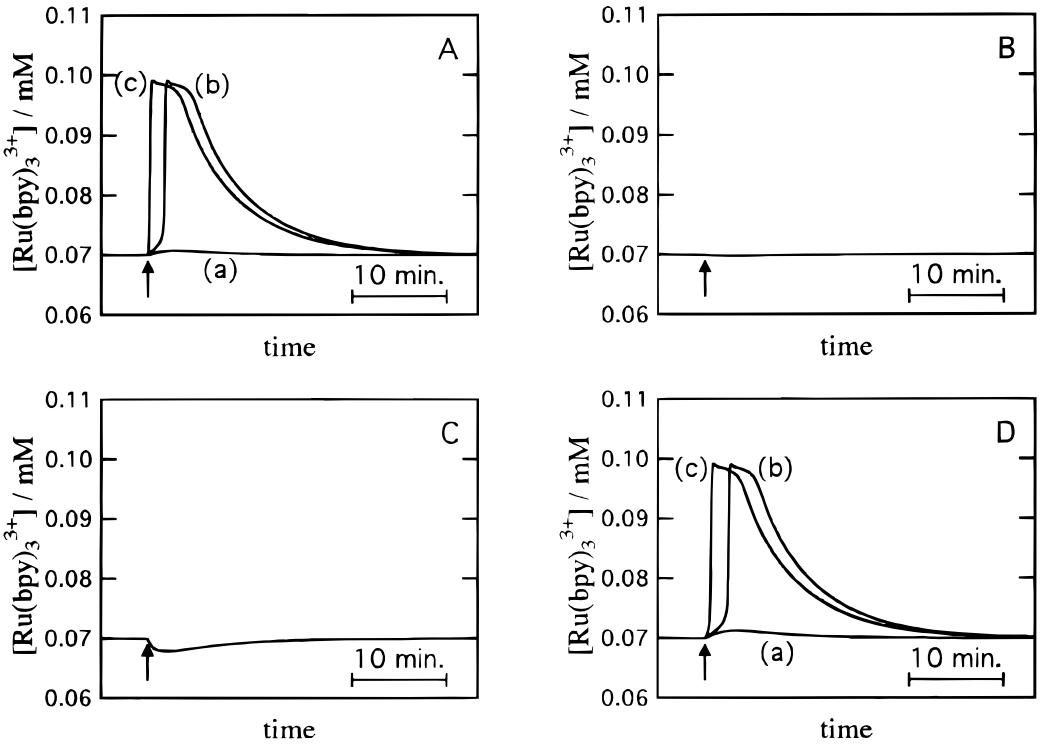

Figure 10. Calculated time profile of $[Ru(bpy)_3^{3+}]$ for the system in SSI after the concentration perturbation. The time of application of the perturbation with a duration of $\tau = 1.0$ s is indicated by an arrow. Initial concentrations are the same as those in Figure 1 except for $[H^+]_0 = 1.0$ M. $k_0 = 1.68 \times 10^{-3}$ s^{-1}. Magnitude of perturbation is $\Delta[HBrO_2] = 1 \times 10^{-7}$ M (A, curve a), 2×10^{-7} M (A, curve b), 1×10^{-6} M (A, curve c), -3.5×10^{-8} M (B), and $\Delta[Br^-] = 1 \times 10^{-4}$ M (C), -6×10^{-7} M (D, curve a), -7×10^{-7} M (D, curve b), 2×10^{-6} M (D, curve c).

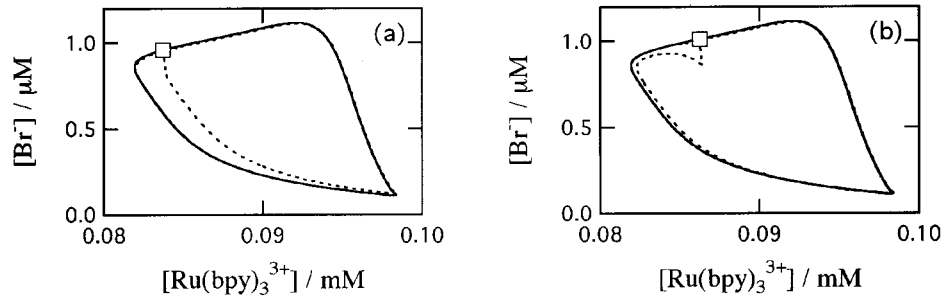

Figure 11. Phase portraits for MBO calculated for the dark oscillations (solid curve) and for the phase-shifted oscillations (broken curve). The time of application of the perturbation ($\Delta[HBrO_2] = 1.5 \times 10^{-7}$ M) with a duration of $\tau = 1.0$ s is indicated by an open square. Panel a is for the phase-advanced case, and panel b is for the phase-delayed case. Initial concentrations are the same as those in Figure 1 except for $[H^+]_0 = 1.0$ M. $k_0 = 1.63 \times 10^{-3}$ s^{-1}.

negative light pulse. These experimental results are all accounted for consistently by the present scheme based on reactions 1−4. Numerical calculations with the NFT model also support our point of view, reproducing the experimental results on the excitability successfully as well as on the phase shift of oscillations.

No evidence was found throughout this work for the photoproduction of Br^-. Even the phase delay observed in the pulse perturbation of the system in OSC could be understood in terms of the photoproduction of $HBrO_2$. This situation is in sharp contrast to the observed phase delay of oscillations in the Br^--added full BZ system in which the malonic acid and Br^- solutions are premixed to increase the concentration of bromomalonic acid.[4,10] In the latter case, the phase delay was observed exclusively at any phase of application of light pulse, indicating the absolute predominance of the photoproduction of Br^- from bromomalonic acid. Under this circumstance, it would be interesting to examine the response of the normal full BZ system to the pulsed light, since the steady light illumination of this system has been examined to show that an increase of P causes bifurcations SSI → OSC → SSI.[5] No SSII (the oxidized steady state) appears in contrast to the present case. It is interesting to see if it would show a similar response to MBO discussed here or to the case of higher concentration of bromomalonic acid. This problem is being studied in our laboratory, and the result will be published in the near future.[25]

Appendix

Recovery of the Br^- Ion Selective Electrode Signal. Suppose the true signal $f(t)$ is deformed because of a delay in the electrode response. Assume the time response of the detector to take the form $\exp(-t/\tau_e)$ where τ_e is the delay time. The observed signal $g(t)$ would be deformed as

$$g(t) = (1/\tau_e)\exp(-t/\tau_e)\int^t \exp(t/\tau_e) f(t)\,dt \qquad \text{(A1)}$$

Therefore, we can estimate the original signal $f(t)$ from

$$f(t) = g(t) + \tau_e[dg(t)/dt] \qquad \text{(A2)}$$

As an example, we may take

$$g(t) = A \sin(\omega t) \tag{A3}$$

Equation A2 gives

$$f(t) = A \sin(\omega t) + \omega \tau_e A \cos(\omega t) \tag{A4}$$

When the time constant of the detector τ_e is much shorter than the oscillation period $T = 2\pi/\omega$,

$$\omega \tau_e = 2\pi \tau_e / T \ll 1$$

holds and eq A4 is a good estimation for the true function $f(t)$. On the other hand, if $\tau_e \gg T$,

$$\omega \tau_e \gg 1$$

which means that the amplitude of the observed signal is of the order of $1/(\omega\tau_e)$ of the true signal. A good signal-to-noise ratio is required to obtain a reliable estimation of $f(t)$.

References and Notes

(1) Vavilin, V. A.; Zhabotinskii, A. M.; Zaikin, A. N. *Russ. J. Phys. Chem.* **1968**, *42*, 1649.
(2) Srivastava, P. K.; Mori, Y.; Hanazaki, I. *Chem. Phys. Lett.* **1992**, *190*, 279.
(3) Hanazaki, I. *J. Phys. Chem.* **1992**, *96*, 5652.
(4) Hanazaki, I.; Mori, Y.; Sekiguchi, T.; Rábai, G. *Physica D* **1995**, *84*, 228.
(5) Mori, Y.; Nakamichi, Y.; Sekiguchi, T.; Okazaki, N.; Matsumura, T.; Hanazaki, I. *Chem. Phys. Lett.* **1993**, *211*, 421.
(6) Tyson, J. J. In *Oscillations and Traveling Waves in Chemical Systems*; Field, R. J., Burger, M., Eds.; Wiley-Interscience: New York, 1985; p 93.
(7) Kuhnert, L. *Nature* **1986**, *319*, 393.
(8) Yamaguchi, T.; Shimamoto, Y.; Amemiya, T.; Yoshimoto, M.; Ohmori, T.; Nakaiwa, M.; Akiya, T.; Sato, M.; Matsumura-Inoue, T. *Chem. Phys. Lett.* **1996**, *259*, 219.
(9) Finkeová, J.; Dolnik, M.; Hrudka, B.; Marek, M. *J. Phys. Chem.* **1990**, *94*, 4110.
(10) Agladze, K.; Obata, S.; Yoshikawa, K. *Physica D* **1995**, *84*, 238.
(11) Sørensen, P. G.; Lorenzen, T.; Hynne, F. *J. Phys. Chem.* **1996**, *100*, 19192.
(12) Grill, S.; Zykov, V. S.; Müller, S. C. *J. Phys. Chem.* **1996**, *100*, 19082.
(13) Kaminaga, A.; Mori, Y.; Hanazaki, I. *Chem. Phys. Lett.* **1997**, *279*, 339.
(14) Kaminaga, A.; Hanazaki, I. *Chem. Phys. Lett.* **1997**, *278*, 16.
(15) Kaminaga, A.; Rábai, G.; Hanazaki, I. *Chem. Phys. Lett.* **1998**, *284*, 109.
(16) Ram Reddy, M. K.; Dahlem, M.; Zykov, V. S.; Müller, S. C. *Chem. Phys. Lett.* **1995**, *236*, 111.
(17) Sekiguchi, T.; Mori, Y.; Okazaki, N.; Hanazaki, I. *Chem. Phys. Lett.* **1994**, *219*, 81.
(18) Boissonade, J.; De Kepper, P. *J. Phys. Chem.* **1980**, *84*, 501.
(19) Noyes, R. M.; Field, R. J.; Thompson, R. C. *J. Am. Chem. Soc.* **1971**, *93*, 7315.
(20) Bar-Eli, K. *J. Phys. Chem.* **1985**, *89*, 2855.
(21) Field, R. J.; Försterling, H.-D. *J. Phys. Chem.* **1986**, *90*, 5400.
(22) Gao, Y.; Försterling, H.-D. *J. Phys. Chem.* **1995**, *99*, 8638.
(23) Robertson, E. B.; Dunford, H. B. *J. Am. Chem. Soc.* **1964**, *86*, 5080.
(24) Rábai, G.; Hanazaki, I. *J. Phys. Chem.* **1996**, *100*, 10615.
(25) Mori, Y.; Kaminaga, A.; Okazaki, N.; Hanazaki, I. To be published.